J. Physiol. (1976), **255**, *pp.* 335–346
With 5 text-figures
Printed in Great Britain

DIRECTIONAL DIFFERENCES OF IMPULSE SPREAD IN TRABECULAR MUSCLE FROM MAMMALIAN HEART

BY L. CLERC

From the Department of Physiology, Bühlplatz 5, 3012 Berne, Switzerland

(*Received 3 February 1975*)

SUMMARY

1. Trabecular bundles from the right ventricle of calf hearts were used. Electrical properties measured by the application of longitudinal current were compared to those measured by the application of transverse current.

2. The following data were obtained on the basis of classical cable analysis: (i) a ratio of 3·0 for longitudinal to transverse conduction velocity, (ii) a ratio of 3·6 for intra- to extracellular longitudinal resistance, (iii) a ratio of 12·6 for intra- to extracellular transverse resistance, (iv) a ratio of 9·4 for intracellular transverse to intracellular longitudinal resistance, (v) a ratio of 2·7 for the extracellular transverse to the extracellular longitudinal resistance.

3. The disparity in conduction velocity could be explained on the sole grounds of differences in the resistivity of the intracellular and extracellular paths for current flow in the two directions, confirming theoretical predictions.

4. The value of the transverse internal resistance can be accounted for on the ground of frequent branching in a three-dimensional network. There is no need to make the additional assumption of current flow through lateral low resistance pathways between parallel fibres.

INTRODUCTION

In an intact mammalian heart the electrical impulse activates the ventricular walls by propagating from the endocardial to the epicardial surface. This has been shown for dog (Scher, Young, Malmgren & Paton, 1953), as well as for human hearts (Durrer, van Dam, Freud, Janse, Meijler & Aerzbacher, 1970) by taking simultaneous records from a great number of recording sites. The result implies that spread of excitation is essentially transverse to the three main anatomical layers of ventricular muscle (Bargmann, 1967). So transverse activation is either mediated by

penetrating fibres of the specific conduction system or occurs through the ventricular fibres. With this latter mechanism in mind it seemed of interest to examine ventricular bundles for their electrical properties, applying current either in the longitudinal or transverse direction. As might be anticipated, transverse propagation is slower. In addition, it will be shown that the ratios of measured conduction velocities agree reasonably well with predictions based on measured resistance of intracellular and extracellular pathways to the flow of activating current.

METHODS

The experiments were performed on calf hearts obtained at the local slaughterhouse and brought to the laboratory in cool Tyrode solution (4° C). Small bundles of trabecular muscle running freely through the cavity of the right ventricle were detached at the ends by fine scissors. Bundles had a length of 5 mm and a diameter of 1·2–1·5 mm. All experiments were carried out at 25° C rather than at 37° C since at this temperature there were no signs of progressive contracture. The composition of Tyrode solution was (mM) Na^+ 149·2, K^+ 5·4, Ca^{2+} 1·8, Mg^{2+} 0·5, Cl^- 146·9, HCO_3^- 11·9, $H_2PO_4^-$ 0·4. The Tyrode was gassed with 95 % O_2, 5 % CO_2. For the longitudinal measurements the bundle was mounted in a chamber as described by Weidmann (1970). Transverse measurements were taken from the same bundle, when transferred to a second chamber. Fig. 1 illustrates the method of mounting the preparation for the transverse recordings. The trabecular muscle was fixed in a 5 mm broad chamber open at the ends. The bundle was slightly squeezed between the Perspex bottom and a rubber membrane which gave it a flatter and broader shape. A slit in the membrane allowed access of the micro-electrodes to the bundle. A layer of silicon oil covering the rubber membrane prevented the bundles from drying out. Tyrode solution flowed in through holes at the bottom of the chamber on both sides of the preparation and escaped through the open ends, thus being in contact with the preparation on both sides. The Tyrode flowing into the four basins at the corners was continually sucked away. Connexion to earth was made through a Tyrode filled channel opening in the middle of the chamber under the preparation.

While the transverse measurements were taken, the Tyrode flow was stopped, so that the surface tension of the water reduced the film at the ends of the bundle to a layer of about 10 μm; taking the specific resistance of Tyrode as 51 Ω cm this would give a shunt current around the ends of less than 1 %. Preparations still showed normal resting and action potentials 12 hr after the standard experiments.

The silicon oil used was Rhodorsil 10^{-2} Stoke, Société des Usines Chimiques Rhône-Poulenc-Paris, Fluide 200.

The recording system consisted of two Ling-Gérard electrodes, filled by the method of Tasaki, Tsukuhara, Ito, Wayner & Yu (1968), two cathode followers and the differential amplifier of a Tektronix oscilloscope (type 502, dual beam).

THEORY

Longitudinal and transverse current flow

The problem is how to describe current flow in heart muscle in the longitudinal and transverse directions. In the case of a super-imposed homogeneous electrical field this requires the application of one-dimensional cable theory and, thus, the real structure of the tissue must be given as an ideal representation. Fig. 2*A* shows a

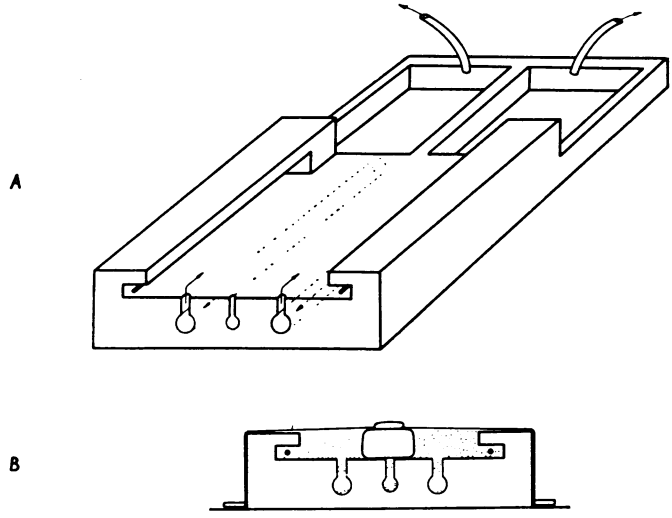

Fig. 1. Chamber used for transverse current flow, viewed obliquely (*A*) and in cross-section (*B*), showing the method of mounting the preparation under a rubber membrane. The slit in the membrane is filled with silicon oil.

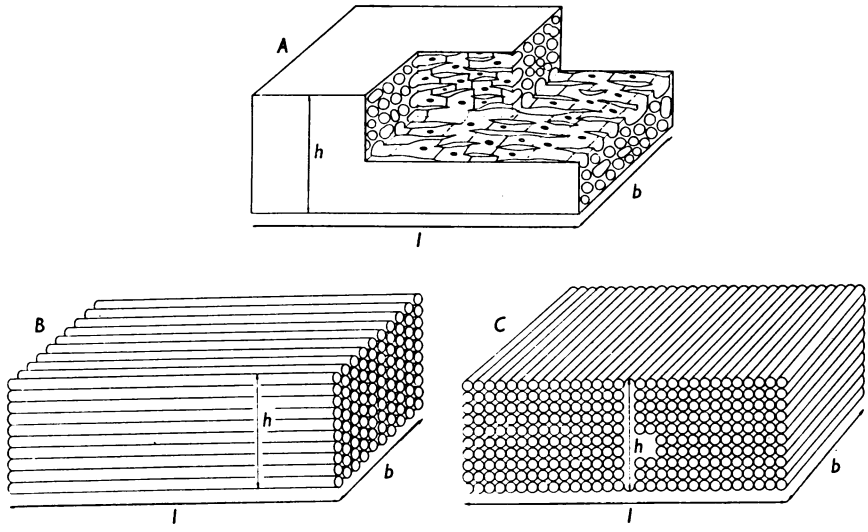

Fig. 2. Side view and cross-section of ventricular trabecular muscle (*A*) showing the frequently branching and reanastomosing three-dimensional structure. *B* is the linear model for longitudinal and *C* for transverse application of a homogeneous electrical field.

relatively realistic picture of the cell connexions. Individual fibres branch and reanastomose, forming a three-dimensional network. The cells are mainly oriented in the longitudinal direction. Intercellular current flow takes place at specialized contacts (nexuses) which are assumed to occur at end-to-end abutments of the cells (see Fig. 2*A*). It is clear that axial current may flow in the longitudinal direction along relatively direct paths. But intracellular current flow in the transverse direction is also possible via tortuous pathways that include the end-to-end contacts and which depends upon the branching structure. A more detailed comparison of longitudinal and transverse current flow is given below.

A one-dimensional cable model for current flow in the longitudinal direction is shown in Fig. 2*B*. The individual fibres are represented by smooth cylinders, oriented longitudinally with radius a (= fibre or cell radius). This idealization allows conventional cable theory to be applied. Details of current flow (the values of sarcoplasmic and nexal resistance, the slight tortuosity in the current path and so on) are reflected in the parameter r_{i_l}. Analogous considerations determine the extracellular resistance per unit length, r_{o_l}.

In the case of transverse propagation the appropriate cable model is less obvious. The correct model can be derived, however, by considering the following geometrical conditions, which apply to a unit volume of tissue: (1) the intracellular and extracellular volumes are fixed quantities, (2) the total surface membrane area is a fixed quantity, these conditions being independent of the direction of current flow. For transverse current flow, the idealized structures must be oriented as shown in Fig. 2*C*. Requirement (1) is satisfied if the structures have the same cross-sectional shape as their longitudinal counterpart (i.e. circular). Requirement (2) insists that the radius of the transverse circular cylinder a_t be equal to the radius of the longitudinal, a. Thus $a_t = a_l = a$. The result is the geometrical arrangement shown in Fig. 2*C*.

The details of the microscopic structure of the tissue have not entered into the model up to this point. However, as in the case of longitudinal propagation, it is the resistance parameters, r_{i_t} and r_{o_t}, which reflect the details of the transverse current flow. Because the tissue is highly anisotropic (see Fig. 2*A*) at the microscopic level, in general $r_{i_t} \neq r_{i_l}$ and $r_{o_t} \neq r_{o_l}$.

Determination of tissue resistivity

The following symbols will be used throughout the paper.

n	number of fibres per unit cross-sectional area
l	longitudinal
t	transverse
x	distance in the longitudinal or in the transverse direction (cm)
τ_{foot}	time constant of foot of propagated action potential (μsec)
V	electrical potential difference resulting from polarizing current (V)
I	polarizing current injected through large electrodes (A)
r_i	inside resistance per unit distance of the bundle (Ω cm^{-1})
r_o	outside resistance per unit distance of the bundle (Ω cm^{-1})
r_j	junctional resistance (Ω cm^{-1})
r_c	cytoplasmic resistance (Ω cm^{-1})
R_i	specific inside resistance (Ω cm)
R_o	specific outside resistance (Ω cm)
c_m	membrane capacity per unit length (F cm^{-1})
C_m	specific membrane capacity of surface membrane (F cm^{-2})
θ	conduction velocity (cm sec^{-1})

a	fibre radius (cm)
mAp_i	monophasic intracellular action potential (mV)
mAp_o	monophasic extracellular action potential (mV)
bAp_i	biphasic intracellular action potential (mV)
bAp_o	biphasic extracellular action potential (mV)
A	point A on the bundle surface or within a cell at a given distance
B	point B on the bundle surface or within a cell at a given distance
L	distance between two branching sites (cm)

Tissue resistance (r_i and r_o in parallel) can be calculated by the equations from Weidmann (1970).

$$\frac{r_i r_o}{r_i + r_o} = \frac{dV}{dx} \Big/ I, \tag{1}$$

$$-\frac{r_i}{r_o} = \frac{mAp_i}{mAp_o}. \tag{2}$$

For practical reasons the actual calculations are based on the comparison of the respective biphasic action potentials,

$$-\frac{r_i}{r_o} = \frac{bAp_i}{bAp_o}, \tag{3}$$

which is derived from (2) on the assumption of a constant r_i/r_o in a given direction, because of the homogeneous structure of the bundle and from the definition

$$bAp_{AB} = mAp_A - mAp_B, \tag{4}$$

specific resistivity is then given by

$$R_i = r_i a^2 \pi . n. \tag{5}$$

Conduction velocity in different directions

The initial part of a propagating action potential shows an exponential time course on theoretical grounds (Tasaki & Hagiwara, 1957; Hodgkin & Huxley, 1952).

$$\tau_{foot} = K^{-1} = \frac{1}{\theta^2 (r_i + r_o) c_m}, \tag{6}$$

or

$$c_m = \frac{1}{\tau_{foot}} \cdot \frac{1}{\theta^2 r_i} \cdot \frac{r_i}{r_i + r_o}, \tag{7}$$

and

$$c_m = C_m . 2 \pi a n. \tag{8}$$

The important point is that τ_{foot} (or its reciprocal k, the propagation constant: Hodgkin & Huxley, 1952) is a function only of the local membrane properties. It is not affected when the conduction velocity is altered by factors which change the current distribution in the fibre without influencing the excitable membrane itself (Hodgkin, 1954). If the same excitable membrane underlies action potential conduction in the longitudinal and transverse direction then,

$$(\tau_{foot})_l = (\tau_{foot})_t. \tag{9}$$

This has been verified experimentally (see Results).

Using eqns. (7) and (8)

$$\theta_l^2 (r_{i_l} + r_{o_l})(2\pi a_l n_l C_{m_l}) = \theta_t^2 (r_{i_t} + r_{o_t})(2\pi a_t n_t C_{m_t}). \tag{10}$$

The one-dimensional model for propagation (Fig. 2 *B, C*) has $a_l = a_t$, $n_l = n_t$. Since C_m is a specific property of the excitable membrane it is reasonable to assume (see Results) that $C_{m_l} = C_{m_t}$. Eqn. (10) then becomes

$$\theta_l^2(r_{i_l} + r_{o_l}) = \theta_t^2(r_{i_t} + r_{o_t}) \tag{11}$$

or

$$\frac{\theta_t}{\theta_l} = \left(\frac{r_{i_l} + r_{o_l}}{r_{i_t} + r_{o_t}}\right)^{\frac{1}{2}}. \tag{11 a}$$

Eqn. (11*a*) may now be tested experimentally.

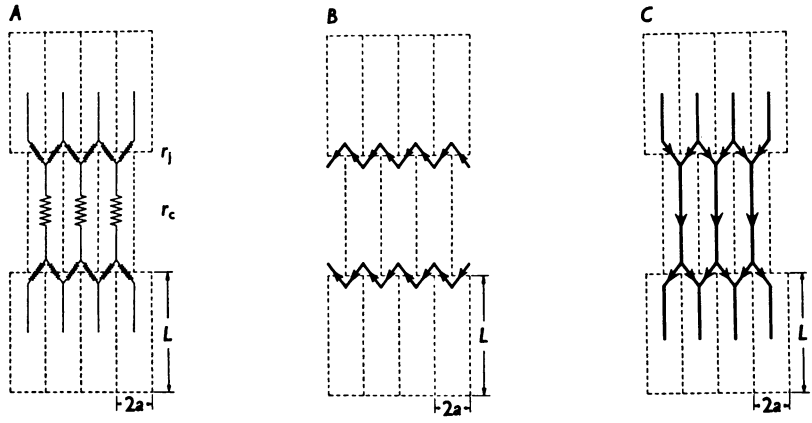

Fig. 3. Schematic two-dimensional model of a ventricular bundle. *A*, arrangement of junctional resistances (r_j) and cytoplasmic resistance (r_c), *B*, pathway for transverse current flow and *C*, pathway for longitudinal current flow. *L* cell length; 2*a* cell diameter.

A simple model for current paths within the cell array

It may be helpful to consider a specific model (Fig. 3 *A* and *B*) of the cell arrangement. This model can be used to calculate the ratio R_{i_t}/R_{i_l}. For simplicity the array of cells is drawn in two dimensions, but similar arguments would apply to a three-dimensional array. Each cell is assumed to make end-to-end contacts of resistance r with four other cells (two at each end). This allows a pathway for transverse current flow (i_t) as well as longitudinal current flow (i_l).

If the resistivity of the sarcoplasm is neglected, the geometrical arrangement of cell contacts is the only determinant of the over-all resistivities in the transverse and longitudinal directions. Then

$$R_{i_t} = \frac{Lr}{2}, \tag{12}$$

$$R_{i_l} = \frac{\pi a^2 r}{2L}, \tag{13}$$

or

$$\frac{R_{i_t}}{R_{i_l}} = \frac{L^2}{\pi a^2}. \tag{14}$$

If the resistivity of the myoplasm is taken into consideration

$$r_i = \frac{B_i}{\pi a^2}; \quad r_c = \frac{R_c}{\pi a^2}; \quad r_j = \frac{nR_j}{\pi a^2}$$

(n = number of junctions per centimetre length), (15)

since $$r_i = r_c + r_j, \tag{16}$$

it follows that $$\frac{R_{i_t}}{R_{i_l}} = \frac{R_{ic_t} + (L^2/\pi a^2)R_j}{R_{ic_l} + nR_j}. \tag{17}$$

The validity of this equation will be discussed below.

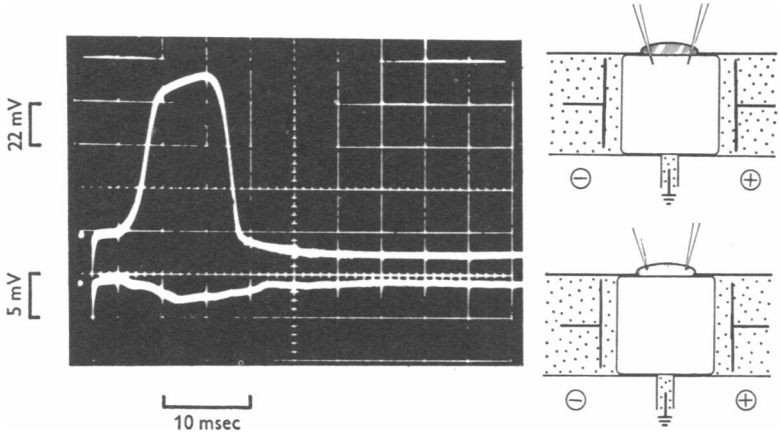

Fig. 4. Method used for estimating r_{i_t}/r_{o_t} from the amplitudes of the intra- and extracellular biphasic action potentials. For further explanation see text.

RESULTS

Tissue resistivity

The longitudinal and transverse resistance of the whole preparation (r_1 and r_0 in parallel) was determined as is shown in Fig. 4 by measuring the voltage gradient near the middle of the bundle during the passage of a 15 msec lasting subthreshold d.c. pulse. The current strength was recorded across a 1 kΩ resistor inserted in series with the electrode system. The average values found were $402 \pm$ S.E. 30 Ω cm in the longitudinal and $3620 \pm$ S.E. 280 Ω cm in the transverse direction; the ratios of r_1 to r_0 were obtained from eqn. (3). Action potentials at a rate of 60 min^{-1} propagating from the cathodal to the anodal end were generated by a suprathreshold 0·7 msec lasting d.c. pulse (cf. Fig. 3). With both micro-electrodes intracellular a differential record was obtained. The electrodes were then withdrawn and a similar extracellular record taken. As was to be expected the deflexions had opposite polarity. If r_1/r_0 were

constant between the recording sites the ratio of the extracellular to the intracellular amplitude should be the same at all times. This expectation was not strictly fulfilled, the records reproduced in Fig. 4 being a particularly bad example. The ratio of the voltage deflexions were taken in a somewhat arbitrary way at the moment when the extracellular record had its maximal amplitude. This must have resulted in an underestimation of r_i/r_o.

The following ratios were found: r_{i_l}/r_{o_l} 3·64 ± S.E. 0·14, r_{i_t}/r_{o_t} 12·7 ± S.E. 1·0, r_{i_t}/r_{i_l} 9·4 ± S.E. 1·0 and r_{o_t}/r_{o_l} 2·69 ± S.E. 0·26.

To calculate the values of R_o, R_i and C_m a cell diameter of 20 μm for calf hearts (Marceau, 1904) and an extracellular space of 30% (Page, 1962) was taken. The values are listed in Table 1.

TABLE 1. Transverse and longitudinal values of the electrical properties of ventricular muscle. + or − S.E. is given in brackets

R_{i_l}	402 ± 30 Ω cm	(9)
R_{i_t}	3620 ± 280 Ω cm	(9)
R_{o_l}	48 ± 4 Ω cm	(9)
R_{o_t}	127 ± 38 Ω cm	(9)
$\tau_{foot}\ l$	640 ± 64 μsec	(13)
$\tau_{foot}\ t$	657 ± 58 μsec	(13)
$C_{foot}\ l$	0·87 ± 0·15 μF cm^{-2}	(8)
$C_{foot}\ t$	0·77 ± 0·10 μF cm^{-2}	(8)
θ_l	48 ± 4 cm sec^{-1}	(9)
θ_t	16 ± 1 cm sec^{-1}	(9)

Conduction velocity

Conduction velocity was measured along and across the bundle in the same arrangement as seen in Fig. 3. The distance between the electrodes was determined by means of a micrometer eyepiece. Time was measured between the midpoints of the rise and fall of the intracellular records. Transverse spread of excitation was slower by a factor of 3·0 ± S.E. 0·2 than longitudinal spread. The absolute values were 16 ± S.E. 1 cm sec^{-1} and 48 ± S.E. 4 cm sec^{-1}, respectively. To check if conduction velocity was constant the electrode distance was varied. A plot of activation time against distance in both longitudinal and transverse direction was reasonably linear suggesting constant propagation velocity.

Quantitative description of directional difference in conduction velocity

The absolute value of the capacity discharged by the propagating action potential was the same when determined by longitudinal or by transverse conduction. This suggests that the directional differences of impulse velocity were only due to the anisotropic behaviour of R_i and

R_0. Theoretically this is described by eqn. (11*a*). The numerical values (average from nine experiments) of the left-hand and right-hand expressions were $3{\cdot}0 \pm$ S.E. 0·6 and $2{\cdot}76 \pm$ S.E. 0·4 respectively which is in good agreement with theory.

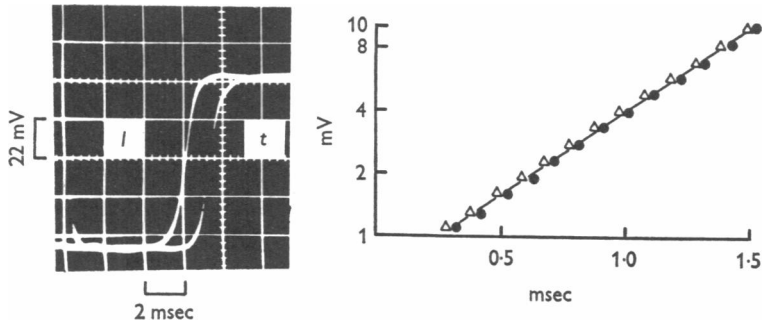

Fig. 5. Measurement of the foot of the propagated action potential. Open symbols for longitudinal and filled symbols for transverse conduction. The time scale on the abscissa is linear, the voltage scale on the ordinate is logarithmic. τ_{foot} can be calculated from the slope of the curve. In this particular case it was 530 μsec for both longitudinal (*l*) and transverse (*t*) propagation.

DISCUSSION

Transverse spread of excitation through mammalian cardiac muscle has been reported by Draper & Mya Tu (1959) and by Sano, Takayama & Shimamoto (1959). It has also been observed with the monolayer heart of a tunicate (Kriebel, 1969) and with smooth muscle (taenia coli; Sperelakis & Prosser, 1959). The ratio of propagation velocities transverse to longitudinal as observed in the present experiments was 1:3 which is in agreement with values as given by Sano *et al.* (1959), 1:5 to 1:2. In the ventricular trabeculae as used for the present experiments, Purkinje fibres are arranged in one or several thin bundles directly underneath the endocardiac layer. It seems unlikely that the specific conduction system is responsible for the pattern of transverse or longitudinal propagation, for at least two reasons, (i) subthreshold depolarizations could be recorded in the fibres closest to the cathode which upon increasing the current strength and reaching an amplitude of 15–20 mV triggered action potentials of a shape typical for ventricular tissue and (ii) impulses invariably propagated from near the cathode to near the anode, reversal of stimulus polarity resulting in reversal of impulse conduction.

There is now general agreement that cardiac cells are connected by low-resistance pathways and that the structure for such pathways is the nexus type junction between adjoining cells (for references see Berger,

1972). Morphometric data in the literature are too incomplete to predict accurate ratios for R_{o_t}/R_{o_l} or R_{i_t}/R_{i_l}. The present model assumes a closed three-dimensional network, in which no lateral tight junctions are present and the intracellular resistance is attributed to the intercellular junctions and to the cytoplasm of the bundle.

The ratio R_{o_t}/R_{o_l} being 2·7 may be explained by the tortuous pathway around tightly packed fibres encountered by transverse current.

On the other hand the high ratio of R_{i_t}/R_{i_l} (9·4) must be connected with the fact that current flowing intracellularly in transverse direction has to take a more closed zig-zag-pathway. The theoretical prediction gives eqn. (17). Marceau (1904) gives a cell diameter in calf ventricle of 20 μm and a cell length of 120 μm. If we assume a specific resistance of cytoplasm equal to 200 Ω cm, a disk resistance of 1 Ω cm^2, and 80 disks per cm we can indeed obtain $R_{i_t}/R_{i_l} = 13{\cdot}7$. The values for myoplasm resistance and disks resistance were chosen to approach the experimental results. The calculation, therefore, has no other significance than to show that reasonable assumptions (see Weidmann, 1966) can indeed account for the ratio R_{i_t}/R_{i_l}.

Berkinblit, Kovalev, Smolyaninov & Chaylakhyan (1971) have pointed out that the distance between neighbouring branching points must be many times shorter than the space constant of a given preparation to allow for sufficient transverse spread of activating current. The space constant in the longitudinal direction of ventricular bundles is reported as 880 μm (Weidmann, 1971). The present model with branching points separated by 120 μm would thus fulfil a prerequisite for transverse conduction as postulated by Berkinblit & Kovalev.

The high value for R_{i_t} as experimentally obtained (3620 Ω cm) can adequately be accounted for by internal current having to take a zig-zag-pathway, crossing cell boundaries at no other sites than at the intercalated disks. Lateral nexuses have been described by various authors (Hama & Kanaseki, 1967; Sommer & Johnson, 1968; Dewey, 1969). However, in the absence of morphometric data their qualitative significance remains doubtful. It must also be pointed out that the nexuses in the intercalated disks are in the longitudinal direction. Thus lateral tight junctions could take part in longitudinal current flow.

Finally it is gratifying to note the following agreement between prediction and results. For widely different external and internal resistances, thus different conduction velocities, the shape of the propagating action potential is the same, as would occur if it was determined exclusively by the properties of the same surface membrane.

My thanks are due to Professor S. Weidmann for suggesting the problem, to Professor A. L. Hodgkin and Dr R. D. Adrian for reviewing the theoretical approach and to Drs R. W. Tsien and J. A. S. McGuigan for reading the manuscript. Financial support was provided by the Swiss National Science Foundation, grant no. 3.758.72.

REFERENCES

BARGMANN, W. (1967). *Histologie und mikroskopische Anatomie des Menschen*, 6th edn, p. 258. Stuttgart: Thieme.

BERGER, W. K. (1972). Correlation between the ultrastructure and function of intercellular contacts. *Electrical Phenomena in the Heart*, ed. DE MELLO, C. New York: Academic Press.

BERKINBLIT, M. B., KOVALEV, S. A., SMOLYANINOV, V. V. & CHAYLAKHYAN, L. M. (1971). The electrical behaviour of the myocardium as a system and the characteristics of the cellular membrane of the heart. *Models of the Structural–Functional Organization of Certain Biological Systems*, ed. GELFAND, I. M., GURFINKEL, V. S., FOMIN, S. V. & ISETLIN, M. L. Cambridge, London: The MIT Press.

DEWEY, M. M. (1969). The structure and function of the intercalated disc in vertebrate cardiac muscle. In *Comparative Physiology of the Heart: Current Trends*, ed. MCCANN, F. V., pp. 10–28. Basel: Birkhäuser.

DRAPER, M. H. & MYA TU, M. (1959). A comparison of the conduction velocity in cardiac tissues of various mammals. *Q. Jl exp. Physiol.* **44**, 91–109.

DURRER, D., VAN DAM, TH., FREUD, G. E., JANSE, M. J., MEIJLER, M. D. & AERZBACHER, R. C. (1970). Total excitation of the isolated human heart. *Circulation* **41**, 899–912.

HAMA, K. & KANASEKI, T. (1967). A comparative microanatomy of ventricular myocardium. In *Electrophysiology and Ultrastructure of the Heart*, ed. SANO, S., MIZUHIRA, V. & MATSUDA, K., pp. 15–26. Tokyo: Bunkodo.

HODGKIN, A. L. (1954). A note on conduction velocity. *J. Physiol.* **125**, 221–224.

HODGKIN, A. L. & HUXLEY, A. F. (1952). A quantitative description of membrane current and its application to conduction and excitation in nerve. *J. Physiol.* **117**, 500–544.

KRIEBEL, M. E. (1969). Spread of excitation and injected current in the tunicate myocardium. In *Comparative Physiology of the Heart: Current Trends*, ed. MCCANN, F. V. Basel and Stuttgart: Birkhäuser.

MARCEAU, F. (1904). Recherches sur la structure et le développement comparé des fibres cardiaques dans la série des vertébrés. *Ann. Sci.* **19**, 191–365.

PAGE, E. (1962). Cat heart muscle in vitro. III. The extracellular space. *J. gen. Physiol.* **46**, 201–213.

SANO, T., TAKAYAMA, N. & SHIMAMOTO, T. (1959). Directional difference of conduction velocity in the cardiac ventricular syncytium studied by microelectrodes. *Circulation Res.* **7**, 262–267.

SCHER, A. M., YOUNG, A. C., MALMGREN, A. L. & PATON, R. R. (1953). Spread of electrical activity through the wall of the ventricle. *Circulation Res.* **1**, 539–547.

SOMMER, J. R. & JOHNSON, E. A. (1968). Cardiac muscle. A comparative study of Purkinje fibres. *J. cell Biol.* **36**, 497–526.

SPERELAKIS, N. & PROSSER, L. (1959). Mechanical and electrical activity in intestinal smooth muscle. *Am. J. Physiol.* **196**, 850–856.

TASAKI, I. & HAGIWARA, S. (1957). Capacity of muscle fibre membrane. *Am. J. Physiol.* **188**, 423–429.

TASAKI, K., TSUKAHARA, Y., ITO, S., WAYNER, M. J. & YU, W. Y. (1968). A simple, direct and rapid method for filling microelectrodes. *Physiol. & Behav.* **3**, 1009–1010.

WEIDMANN, S. (1966). The diffusion of radiopotassium across intercalated disks of mammalian cardiac muscle. *J. Physiol.* **187**, 323–342.

WEIDMANN, S. (1970). Electrical constants of trabecular muscle from mammalian heart. *J. Physiol.* **210**, 1041–1054.